كلية الهندسة بشبرا
FACULTY OF ENGINEERING AT SHOUBRA
ERJ
PRINT ISSN 3009-6049
ONLINE ISSN 3009-6022

ENGINEERING RESEARCH JOURNAL (ERJ)
Volume (53) Issue (4)
October. 2024, pp:193-200
https://erjsh.journals.ekb.eg

Swelling potential and shrinkage potential of stabilized swelling soil using fine sand and fiber through wetting and drying cycles

Mohamed Elsayed AbouRaya[1]*, Nasser Mosleh Saleh[2], Alnos Ali Hegazy[2], Amani Gouda Salama[2]

[1]Higher Institute of Engineering, 6th October City.

[2]Department of Civil Engineering, Faculty of Engineering at Shoubra, Benha University, Cairo, Egypt.

* Corresponding Author.

E-mail: mohamed.abdelazeem18@feng.bu.edu.eg, nasser.saleh@feng.bu.edu.eg, alnnos.hegazy@bhit.bu.edu.eg, amani.ali@feng.bu.edu.eg

Abstract: Clay soils, particularly swelling soils, have long been a significant concern for geotechnical engineers. In this study, the swelling potentials during wetting cycles and the shrinkage potentials during drying cycles were investigated. These cycles were simulated using a specially manufactured model designed to simulate natural conditions. The simulated tests were conducted on remolded specimens collected from a site near Cairo, Egypt. Additionally, the simulated tests were conducted to investigate the effects of adding fine sand and fiber with different proportions to the swelling soil. The specimens used in the simulation tests were prepared and placed in specimen rings with maximum dry density and optimum moisture content. The results showed that there is a reduction in the swelling potential and shrinkage potential with an increasing number of cycles until equilibrium is reached. The test results show that the greatest reduction in swelling potentials for all specimens occurred after the first cycle. During the first wetting cycle, the swelling potential reduced from 29.35% to 23.55% with the addition of fine sand and from 29.35% to 18.75% with the addition of fibers. Similarly, during the first drying cycle, the shrinkage potential reduced from 13.80% to 13.23% with the addition of fine sand and from 13.80% to 9.56% with the addition of fibers. The fibers used in this study were obtained by shredding expired car tires into small pieces.

Keywords **:** Swelling soil; wetting and drying cycles; swelling and shrinkage potential.

1. INTRODUCTION

Swelling soil is renowned as one of the most problematic soil types. It is characterized by its tendency to undergo notable volume changes in response to variations in moisture content, often leading to ground deformation. When inundated, it swells, weakening shear strength, or develops swelling pressure if swelling is prevented. In dry conditions, it shrinks, forming cracks. Consequently, lightweight structures such as roadways, pipelines, and bridges constructed on swelling soils tend to be damaged as a result of deformation [1], [2]. The damage resulting from the impact of swelling soil on these lightweight civil engineering structures is more than twice the damage caused by combined natural disasters, such as floods and earthquakes [3]. The damage caused by swelling soil has been noted in several countries, resulting in significant financial losses, often amounting to millions of dollars, due to structural damage. The expenses associated with maintenance and repairs can frequently exceed the initial foundation costs[4]. Swelling soil is widespread globally, particularly in regions with alternating dry and wet seasons. It is found in various parts of the world [5], including many areas of Egypt [6]. The swell potential of swelling soil can be influenced by soil properties, environmental factors, or the existing state of stress on the soil. Montmorillonite is the primary clay mineral associated with soil volume changes, although kaolinite can also induce volume changes when particle sizes are very fine [7]. Due to the widespread of swelling soil and the significant damage it causes to engineering structures, researchers in geotechnical engineering have found solutions to this problem, while continuing their research efforts aimed at solving it.

The purpose of physical and mechanical stabilization is to minimize swelling pressure without amending its chemical composition [8]. Several physical and mechanical methods can stabilize swelling soil, including soil replacement, blending with non-swelling materials, pre-wetting,

compaction, wetting-drying cycles, and soil reinforcement. This study utilizes wetting-drying cycles for stabilization, as well as blending swelling soil with fine sand and fiber.

Some researchers have used sand to improve the properties of swelling soil. An experimental program was conducted to understand how adding sand stabilizes swelling soil through mixing and layering. The study analyzes the impact of adding sand on soil consistency, showing significant improvement. Additionally, it examines how sand additives mitigate swelling, reducing the lifting of structures. The study indicates that the reduction in swelling is attributed to the lower clean density of the clay in clay-sand mixture [9].

Although the wetting and drying method is not typically recognized as a direct mechanical stabilization technique, it can be utilized to reduce the swelling behavior of swelling soils in specific civil engineering projects, such as canal construction. Several studies have employed this method. Based on their results, conducting successive swell-shrink cycles, where shrinkage involves drying a soil sample below its shrinkage limit, may result in either an increase or decrease in swelling potential [10]–[12].

2.Experimental program

The main objective of the experimental program is to study the change in the volume of the swelling soil used in this study during wetting and drying cycles, as well as to examine the effect of adding fine sand and fiber in different proportions. A modified Proctor test was conducted, with samples prepared to simulate the studied cycles. Additionally, a free swelling test was performed on all samples to evaluate the impact of adding both sand and fiber. The liquid limit and plastic limit tests were also conducted on the swelling soil sample, as well as on samples with added sand.

2.1 Materials used in this study

2.1.1Swelling soil

The swelling soil used was collected from a site in Kafr Hamied, a village affiliated with the Al-Ayat Center in the Giza Governorate, Egypt. The disturbed soil samples, obtained from a depth of three meters below the ground surface, exhibit a light gray color with slight traces of brown. The collected samples were transported to the lab for testing. The samples were air-dried, pulverized, and sieved through a 0.425 mm (No. 40) sieve. The soil was then mixed for homogeneity and stored in closed plastic bags. This soil was selected due to its very high swelling potential, as indicated by indirect inferential testing methods through the engineering properties of the originally tested soil, as shown in Table 1. Additionally, mineralogical identification methods, including X-ray diffraction analysis (XRD) of the soil, were conducted at the national research center in Dokki, and the results are presented in Table 2. The (XRD) results indicate the presence of main clay minerals: montmorillonite, kaolinite, calcium stearate, and zeolite.

Table 1: Properties of the original tested swelling soil

Engineering Properties	Value
Liquid Limit (%)	102
Plastic Limit (%)	47
Plasticity Index (%)	55
Unified Soil Classification System(USCS)	MH
AASHTO [a] Classification System	A-7-5
Maximum Dry density (MDD) (gm./cm^3)	1.61
Optimum Moisture Content (OMC) (%)	20.6
Specific Gravity (G_s)	2.65
Free Swelling (%)	168.3

[a] American Association of State Highway and Transportation Officials

Table 2: X-ray diffraction analysis (XRD) of the original swelling soil

Mineral Name	Semi-Quantitative [%]
Montmorillonite-(Cs)	48.5
Kaolinite 2M	29.3
Calcium Squarate	16.2
Zeolite	6.1

2.1.2 Sand

The sand used in this study is fine sand obtained from 6th of October City. It was sieved to pass through the 0.475 mm (No. 40 sieve) and retained on the 0.075 mm (No. 200 sieve) as per ASTM standards [13]. The particle size distribution curve for fine sand is shown in Figure 1. The engineering properties of fine sand are detailed in Table 3. This fine sand is utilized as a soil stabilizer.

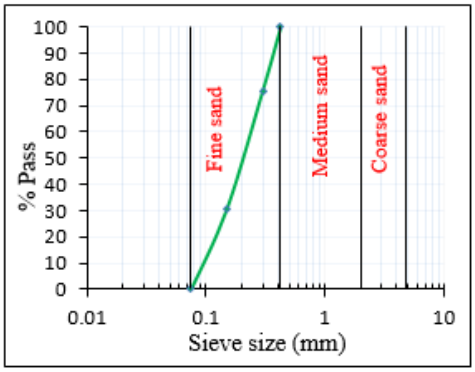

Fig 1 Particle size distribution curve for fine sand

Table 3: Engineering properties of fine sand

Properties	Value
Effective diameter D_{10}(mm)	0.095
D_{30}(mm)	0.150
D_{60}(mm)	0.250
Uniformity coefficient (C_u)	2.360
Coefficient of curvature(C_c)	0.950
USCS classification	SP
Specific Gravity	2.69

2.1.3Fiber

The fiber utilized in this study was obtained by breaking up expired car tires into small parts and passing them through a 4.75 mm sieve (No. 4). A specific gravity test and a sieve analysis test were conducted on the fiber to determine its physical properties. The particle size distribution curve for fiber is shown in Figure 2. The physical and chemical composition of fibers is detailed in Table 4. This fiber is used as a soil stabilizer.

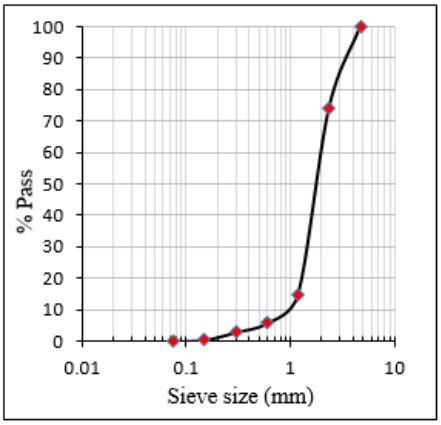

Fig 2 Particle size distribution curve for fiber

Table 4: Fiber's physical and chemical composition

Properties	Value	Properties	Value
Specific Gravity (G_s)	1.01	Water adsorption (%)	26.5
Effective diameter D_{10}(mm)	1.00	Rubber ratio (%)	60
D_{30}(mm)	1.60	Carbon black (%)	35
D_{60}(mm)	2.00	Zinc oxide (%)	2
Uniformity coefficient (C_u)	2	Organic matters (%)	2
Coefficient of curvature(C_c)	1.28	Sulphur (%)	1
Solubility in water	Insoluble		

2.2Wetting and drying Cycles simulation

2.2.1Apparatus Components.

The wetting and drying cycles are simulated to natural conditions using some modifications on conventional oedometer apparatus, similar to those described in references [11], [12]. The modified apparatus consists of a specimen ring with a diameter of 50 mm and a height of 20 mm, along with a bottom porous stone, an upper porous stone, and an outer ring for fixation. A load plate supports the loads and is equipped with vents for water access to the specimen. A strain dial gauge with a precision of 0.01 mm measures axial deformations. A drainage path with a valve aids in water removal. Temperature control, achieved by a heating coil connected to the temperature controller unit (TCU), regulates the drying process. The apparatus is connected to power. Figures 3 and 4 illustrate the details of its components and the wetting and drying simulation cycles apparatus photo, respectively.

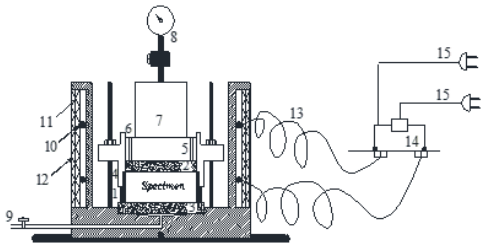

1. Specimen ring.
2. Top porous stone.
3. Bottom porous stone.
4. Outer ring.
5. Load plate.
6. Vents.
7. Load.
8. Strain dial gauge.
9. Valve.
10. Heating coil.
11. Insulation rolls.
12. Metal cover.
13. Wire.
14. Temperature controller unit
15. Power supply

Fig 3: Components of the modified oedometer

Fig 4: Modified oedometer apparatus

2.2. Specimens preparation

Seven groups of remolded soil samples were used in the study: (G), (GS1), (GS2), (GS3), (GF1), (GF2), and (GF3). To prepare the remolded original specimens (G), first, obtain a specimen of swelling soil from previously prepared plastic bags. Then, dry the soil in an oven at 105-110°C for 24 hours. Next, finely pulverize the dried soil and pass it through a 0.425 mm (No. 40) sieve. After that, mix the pulverized soil with distilled water until it reaches the optimum moisture content (OMC) determined from the modified Proctor test.

Finally, store the mixture in a closed bag for 24 hours to ensure the homogeneity of the specimen.

To prepare remolded specimens (GS1), (GS2), and (GS3), follow the original specimen (G) preparation steps, except after sieving, add 5%, 10%, and 15% fine sand based on the swelling soil's dry weight, respectively.

To prepare remolded specimens (GF1), (GF2), and (GF3), follow the original specimen (G) preparation steps, except after sieving, add 5%, 10%, and 15% fiber based on the swelling soil's dry weight, respectively.

2.2.3Test procedure.

The plastic bag is opened, and the sample is extracted. It is then placed in the ring and compacted until reaching the maximum dry density (MDD). A strain dial gauge is used to measure axial deformations. Throughout all experiments, a consistent surcharge pressure of 0.05 kg/cm^2 (5 kPa) is applied by both the load and load plate.

Leave the specimen to swell under surcharge pressure by closing the valve and filling the cell with distilled water to start the wetting process. Measure the axial deformation until the rate of change is 0.02 mm in 24 hours. Record the final vertical deformation at the end of the wetting process. Then, open the valve to drain the water.

Activate temperature control at 42±2°C. This temperature was chosen based on the average of the highest temperatures recorded at the sampling site in the summer of 2020 by Egyptian Meteorological Authority management of climate data. To start the drying process, allow the specimen to dry under surcharge pressure and constant temperature. Monitor axial deformation until the rate of change reaches 0.02 mm within a 24-hour period. Record the final vertical deformation at the end of the drying process.

A single wetting and drying cycle consists of the wetting process followed by a subsequent drying process, and this one cycle takes approximately one week. Upon finishing the wetting and drying cycle, a waiting period of 2-3 hours between wetting and drying cycles takes place until the specimen temperature returns to room temperature [12].

The swelling or shrinkage potential for any cycle was determined using the following equation [14] :

$$S_p\,(N) \text{ or } SH_p\,(N) = \frac{\Delta Hu(N)}{H_0\,(N-1)} \quad N = \{1, 2, 3\ldots\}. \qquad (1)$$

Where:

- **S_p (N):** Swelling potential for the Nth wetting cycle.
- **SH_p (N):** Shrinkage potential for the Nth drying cycle.
- **ΔH_u(N):** Ultimate change in the sample's thickness during the Nth wetting or drying cycle.
- **H_o(N-1):** Initial thickness before the start of the Nth wetting or drying cycle.

3Results and discussion

3.1 Free Swell.

The procedures outlined by the Egyptian Code [15] and Holtz and Gibbs [16] were utilized in this study to determine the free swell for specimens (G, GS1, GS2, GS3, GF1, GF2, and GF3). The free swell results are shown in Figure 5, and the values of free swell are listed in Table 5. The reason for enhancing the free swell with both fine sand and fiber was to replace a swelling material with a non-swelling material. The enhancement with fiber was greater than that with fine sand because the specific gravity of fiber is less than that of fine sand. Consequently, fiber occupies a larger volume than sand.

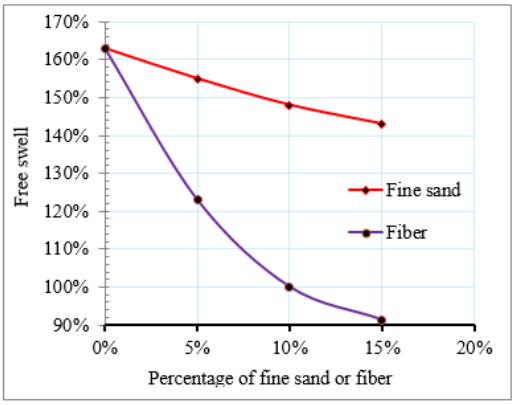

Fig 5: Free swell test results

Table 5: Free swell test results

Soil Specimen	G	$G.S_1$	$G.S_2$	$G.S_3$	$G.F_1$	$G.F_2$	$G.F_3$
Free swell, (%)	163.3	155.0	148.0	143.0	123.0	100.0	91.30
Enhancement, (%)	----	13.3	20.3	25.3	45.3	68.3	77.0

3.2 Liquid limit and plastic limit.

Liquid limit and plastic limit tests were performed on (G, GS1, GS2, GS3, GF1, GF2, and GF3) in accordance with the Egyptian code of practice [17] and ASTM-D4318 [18]. Table 6 shows these results. From the results, increasing the percentage of fine sand in the swelling soil decreased both liquid and plastic limits, as observed. Additionally, this increase led to a decrease in the plasticity index, as shown in Figure 6. The reduction in fines content, which contributes to plasticity, is due to the increase in the proportion of sand. Both the liquid limit and plasticity index decrease with the addition of fine sand.

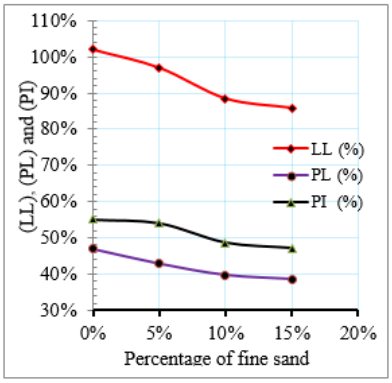

Fig 6: The effect of fine sand addition on liquid limit, plastic limit, and plasticity index.

Table 6: liquid limits, plastic limits and plasticity index results

Soil Specimen	liquid limits (L.L)	plastic limits (P.L)	plasticity index (P.I)
G	102.0%	46.9%	55.1%
$G.S_1$	97.0%	42.9%	54.1%
$G.S_2$	88.5%	39.8%	48.7%
$G.S_3$	85.9%	38.7%	47.2%

3.3The results of compaction test.

The modified compaction test was performed on seven remolded soil specimens (G, GS1, GS2, GS3, GF1, GF2 and GF3) to find the optimum moisture content (OMC) needed to achieve maximum dry density (MDD) under modified compaction energy. The test procedures were conducted following the Egyptian code of practice [17] and ASTM D1557 method 'A' [19]. The results of this test are significant for preparing specimens to simulate wetting and drying cycles.

Figure 7 and Table 7 illustrate the effect of adding different proportions of fine sand and fiber to swelling soil on the OMC and MDD. Based on the previous results, it was observed that the (MDD) decreased with an increasing proportion of added fiber. This can be explained by the fibers dispersing and absorbing some of the compaction effort, their high tensile strength resisting the sliding of soil particles, and their low specific gravity [20].

Table 7: **The results of the modified Proctor tests**

Soil Specimen	G	$G.S_1$	$G.S_2$	$G.S_3$	$G.F_1$	$G.F_2$	$G.F_3$
MDD, (gm/cm^3)	1.61	1.648	1.67	1.69	1.49	1.43	1.40
OMC, (%)	20.6	19.8	19.2	19.0	25.0	25.0	25.5

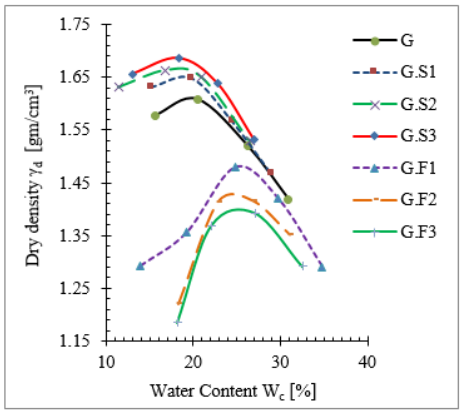

Fig 7: **The results of the modified Proctor tests**

3.4 Swelling and shrinkage potential

Figures 8 and 9 show the swelling potentials during five wetting cycles for soil treated with sand (G, GS1, GS2, and GS3) and fiber (G, GF1, GF2, and GF3), respectively. Additionally, Figures 10 and 11 show the shrinkage potentials during five drying cycles for soil treated with sand (G, GS1, GS2, and GS3) and fiber (G, GF1, GF2, and GF3), respectively, compared to the control specimen (G).

Tables 8 and 9 show the test results for swelling and shrinkage, respectively.

Table 8: Swelling potential values during wetting cycles

Soil Specimen	Swelling potential during wetting cycles, (%)				
	1st cycle	2nd cycle	3rd cycle	4th cycle	5th cycle
G	29.35	21.52	21.02	20.95	20.99
$G.S_1$	24.45	20.35	20.04	19.53	19.65
$G.S_2$	24.10	19.31	19.67	19.15	19.23
$G.S_3$	23.55	19.22	19.16	18.47	18.52
$G.F_1$	23.50	18.79	16.49	17.97	17.92
$G.F_2$	19.50	16.36	15.07	16.86	16.99
$G.F_3$	18.75	12.66	13.73	16.38	16.34

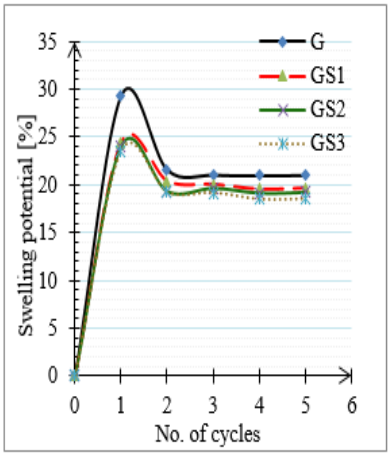

Fig 8: **The swelling potential through five wetting cycles for G, GS_1, GS_2, and GS_3 specimens.**

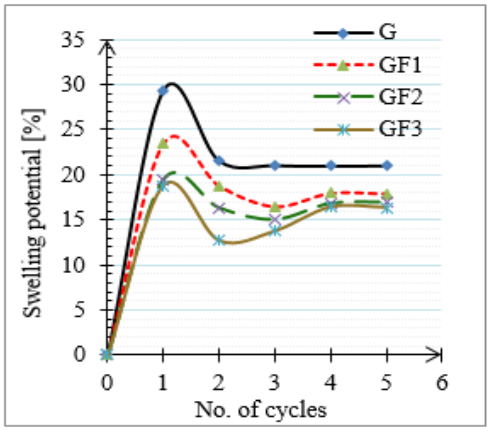

Fig 9: The swelling potential through five wetting cycles for G, GF_1, GF_2, and GF_3 specimens.

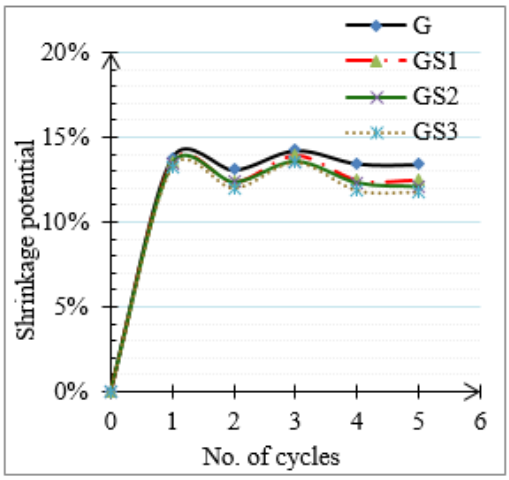

Fig 10: The shrinkage potential through five drying cycles for G, GS_1, GS_2, and GS_3 specimens

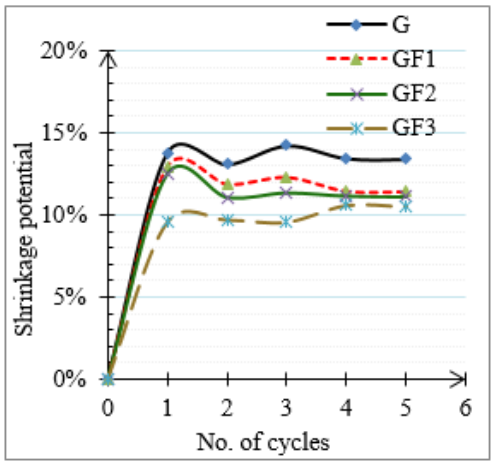

Fig 11: The shrinkage potential through five drying cycles for G, GF_1, GF_2, and GF_3 specimens.

Table 9: **Shrinkage potential values during drying cycles**

Soil Specimen	Shrinkage potential during drying cycles, (%)				
	1st cycle	2nd cycle	3rd cycle	4th cycle	5th cycle
G	13.80	13.10	14.25	13.46	13.41
$G.S_1$	13.54	12.36	13.94	12.49	12.50
$G.S_2$	13.42	12.36	13.57	12.31	12.09
$G.S_3$	13.23	12.01	13.54	11.88	11.79
$G.F_1$	12.96	11.90	12.32	11.47	11.45
$G.F_2$	12.51	11.10	11.37	11.17	11.12
$G.F_3$	9.56	9.71	9.58	10.59	10.51

The previous results illustrated in Table 8 and Table 9, for both swelling potential and shrinkage potential through swelling and shrinkage cycles, show a reduction in both swelling potential and shrinkage potential with advancing cycles. The reason for this is that the soil microstructure undergoes reconstruction after each cycle. In addition, strong van der Waals bonds are able to assemble and cement swelling soil particles. These bonds are generated due to capillary pressures after the drying cycle. The results agree with those of Yazdandoust and Yasrobi [21].

From the previous results, the maximum vertical deformation differences in one cycle are observed at the first cycle for all specimens. The equilibrium state of vertical deformation was observed after the fourth cycle for all specimens as agreed with Yazdandoust and Yasrobi [21].

The axial vertical deformation differences between swelling potential and shrinkage potential in the 1st and 5th cycles are illustrated in Table 10 and Figures 12 and 13.

Table 10: The Axial vertical deformation difference in 1st and 5th cycle

Soil Specimen	Axial vertical deformation difference, (%)	
	1st cycle	5th cycle
G	15.55	7.53
$G.S_1$	10.91	7.09
$G.S_2$	10.68	6.99
$G.S_3$	10.32	6.66
$G.F_1$	10.54	6.48
$G.F_2$	6.99	5.78
$G.F_3$	9.19	5.80

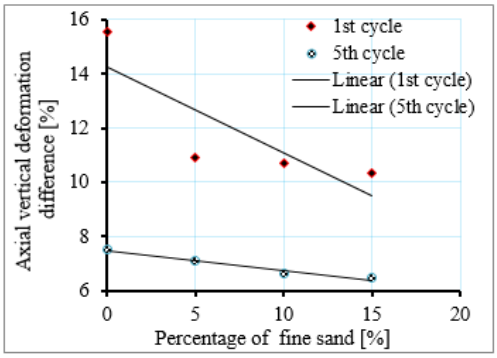

Fig 12: Axial vertical deformation difference in 1st and 5th cycle for G, GS_1, GS_2, and GS_3 specimens.

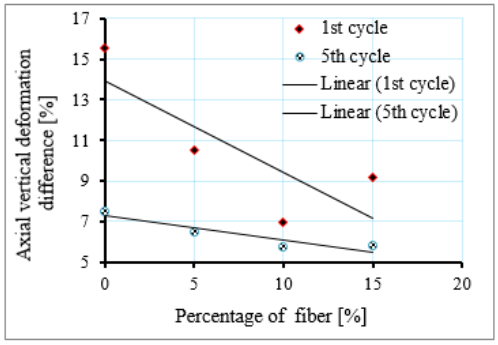

Fig13: Axial vertical deformation difference in 1st and 5th cycle for G, GF1, GF2, and GF3 specimens.

4.Conclusion

Two mechanical stabilization methods for swelling soil are used in this study. The first method involves wetting-drying cycles, while the second method includes blending fine sand or fiber with the swelling soil. Additionally, the two methods were also combined for further analysis.

As for the mechanical stabilization method involving wetting and drying cycles for specimen (G), it resulted in a reduction in the swelling potential value from 29.35% during the first wetting cycle to 20.99% by the fifth wetting cycle. Similarly, there was a slight decrease in the shrinkage potential value from 13.80% during the first drying cycle to 13.46% by the fifth drying cycle. Consequently, the maximum vertical deformation differences within one cycle decreased from 15.55% during the first cycle to 7.53% after reaching the equilibrium state.

Blending fine sand with the swelling soil reduced the liquid limit from 102.0% to 85.9% and the plastic limit from 46.9% to 38.7%, consequently decreasing the plasticity index from 55.1% to 47.2%. Additionally, the free swell decreased from 168.3% to 143%. On the other hand, blending fiber with the swelling soil reduced the free swell from 168.3% to 91.3%.

Regarding the combined use of both methods, the following conclusions can be drawn: the maximum vertical deformation differences decreased from 15.55% to 10.32% with the addition of 15% fine sand and from 15.55% to 6.99% with the addition of 10% fiber, all observed in the first cycle. Additionally, the axial vertical deformation difference between swelling and shrinkage after reaching equilibrium decreased from 7.53% to 6.66% with the addition of 15% fine sand and from 7.53% to 5.78% with the addition of 10% fiber.

References

[1] T. Schanz and M. B. D. Elsawy, "Stabilisation of highly swelling clay using lime–sand mixtures," *Proc. Inst. Civ. Eng. Gr. Improv.*, vol. 170, no. 4, pp. 218–230, 2017, doi: 10.1680/jgrim.15.00039.

[2] B. Devkota, M. R. Karim, M. M. Rahman, and H. B. K. Nguyen, "Accounting for Expansive Soil Movement in Geotechnical Design—A State-of-the-Art Review," *Sustain.*, vol. 14, no. 23, pp. 1–27, 2022, doi: 10.3390/su142315662.

[3] M. Mokhtari and M. Dehghani, "Swell-Shrink Behavior of Expansive Soils, Damage and Control," *Electron. J. Geotech. Eng.*, vol. 17, pp. 2673–2682, 2012.

[4] M. Zumrawi, A. ElfatihA Gameil, M. M. E Zumrawi, A. O. Abdelmarouf, and A. E. A Gameil, "Damages of buildings on expansive soils:- diagnosis and avoidance," *Int. J. Multidiscip. Sci. Emerg. Res.*, vol. 6, no. 2, pp. 108–116, 2017, [Online]. Available: http://www.ijmser.com/.

[5] B. Kalantari, "Foundations on expansive soils: A review," *Res. J. Appl. Sci. Eng. Technol.*, vol. 4, no. 18, pp. 3231–3237, 2012.

[6] E. A. El-Kasaby, A. A. Easa, M. F. Abd-Elmagied, and M. G. El-Abd, "Experimental study of expansive soil in new urban areas surrounding Cairo," *Eng. Res. J. Fac. Eng. Menoufia Univ.*, vol. 42, no. 1, pp. 49–59, 2019.

[7] O. BAŞER, "Stabilization of expansive soils using waste marble dust," middle east technical university, 2009.

[8] J. A. H. Carraro, J. Dunham-friel, and M. Smidt, "Beneficial use of scrap tire rubber in low-volume road and bridge construction with expansive soils," Colorado State University, 2010.

[9] B. Louafi and R. Bahar, "Sand: An Additive for Stabilzation of Swelling Clay Soils," *Int. J. Geosci.*, vol. 3, pp. 719–725, 2012.

[10] A. Soltani, A. Taheri, M. Khatibi, and A. R. Estabragh, "Swelling Potential of a Stabilized Expansive Soil: A Comparative Experimental Study," *Geotech. Geol. Eng.*, vol. 35, no. 4, pp. 1717–1744, 2017, doi: 10.1007/s10706-017-0204-1.

[11] S. Shahsavani, A. H. Vakili, and M. Mokhberi, "The effect of wetting and drying cycles on the swelling-shrinkage behavior of the expansive soils improved by nanosilica and industrial waste," *Bull. Eng. Geol. Environ.*, vol. 79, no. 9, pp. 4765–4781, 2020, doi: 10.1007/s10064-020-01851-6.

[12] A. R. Estabragh, B. Parsaei, and A. A. Javadi, "Laboratory investigation of the effect of cyclic wetting and drying on the behaviour of an expansive soil," *Soils Found.*, vol. 55, no. 2, pp. 304–314, 2015, doi: 10.1016/j.sandf.2015.02.007.

[13] A. C. D.-18 on Soil and Rock, "Standard Practice for Classification of Soils for Engineering Purposes (Unified Soil Classification System) 1," vol. i, 2017.

[14] A. Soltani, A. Deng, A. Taheri, M. Mirzababaei, and S. K. Vanapalli, "Swell-shrink behavior of rubberized expansive clays during alternate wetting and drying," *Minerals*, vol. 9, no. 4, pp. 1–18, 2019, doi: 10.3390/min9040224.

[15] HBRC, *Egyptian Code for Soil Mechanics—Design and Construction of Foundations, Part 5, 5/202 Foundations on problematic soil Code No. 202-2001*, 2012th ed. CAIRO EGTPT, 2001.

[16] W. G. Holtz and H. J. Gibbs, "Engineering Properties of Expansive Clays," *Trans. Am. Soc. Civ. Eng.*, vol. 121, no. 1, pp. 641–663, Jan. 1956, doi: 10.1061/TACEAT.0007325.

[17] HBRC, *Egyptian Code for Soil Mechanics—Design and Construction of Foundations, Part 2, 2/202 Laboratory Experiments Code No. 202-2001*, 2018th ed. CAIRO EGTPT, 2001.

[18] ASTM International, "Standard Test Methods for Liquid Limit, Plastic Limit, and Plasticity Index of Soils ,ASTM D4318-10e1," 2014.

[19] ASTM International, "Standard Test Methods for Laboratory Compaction Characteristics of Soil Using," *ASTM Stand. Guid.*, vol. 3, pp. 1–10, 2003, doi: 10.1520/D1557-12.1.

[20] C. Gelder and G. J. Fowmes, "Mixing and compaction of fibre- and lime-modified cohesive soil," *Proc. Inst. Civ. Eng. Gr. Improv.*, vol. 169, no. 2, pp. 98–108, 2016, doi: 10.1680/grim.14.00025.

[21] Fateme Yazdandoust and S. S. Yasrobi, "Effect of cyclic wetting and drying on swelling behavior of polymer-stabilized expansive clays," *Appl. Clay Sci.*, vol. 50, no. 4, pp. 461–468, 2010.